**ILL Number: 67442490**

**BLC**

**Shipping Method: Ariel**

**Yes No Cond**

**Borrower: UCW**

**In Process:** 20100721

**Lending String: *MYG,NRC,UMC,OKU,GAT**

**Patron:** Savkar, Amit

**Journal Title:** Reliability, packaging, testing, and characterization of MEMS/MOEMS IV ; 24-25 January 2005, San Jose, California, USA /

**Volume:** 5716 **Issue:** 1
**Month/Year:** January 2005
**Pages:** 158-164

**Article Author:**

**Article Title:** Dynamic excitation; a noninvasive technique for initiating stiction repair in MEMS;

**Borrowing Notes:** Billing Notes; FEIN 06-6000798 / CISTI; FGH82127 / BRI; 51-9055 / CAS; 5004885

**OCLC#** 59132052

**Imprint:** Bellingham, Wash. ; SPIE, c2005.

**Call #: att**

**Charge:**

**MaxCost: $75IFM**

**Library Address:**
Univ of Connecticut
Babbidge Library
DD-ILL Office (U-2005F)
369 Fairfield Way

**Shipping Address:**

**Fax:** 860-486-3593
**Email Address: udoc@uconn.edu**

**Request Type:** Article
**Document Type:**





**Ariel Address: 137.99.96.19**

# Dynamic excitation- a noninvasive technique for initiating stiction repair in MEMS

A.A. Savkar†, K.D. Murphy*†, and M.R. Begley§

†Division of Applied Mechanics
Department of Mechanical Engineering
University of Connecticut, Storrs, CT 06269-3139

§Structural and Solid Mechanics Program
Department of Civil Engineering
University of Virginia, Charlottesville, VA 22904-4742

## ABSTRACT

Commercial applications of micro-electromechanical systems (MEMS) continue to be plagued by reliability issues encountered during fabrication and operation. One of the most prevalent problems is the adhesion between adjacent components since adhesive forces are known to promote wear and defect-related failures. In extreme circumstances, the adhesion is large enough to prevent separation, a phenomenon commonly referred to as *stiction-failure*. The objective of current work is to determine analytically whether dynamic excitation may be used to repair stiction-failed cantilevers. This is accomplished by relating the structural dynamic response to the de-cohesion of stiction-failed micro-cantilever beams under various loading conditions.

## 1. INTRODUCTION

A typical schematic of such a failed micro-cantilever beam is shown in Figure 1a. Modal analysis is used to describe the dynamic response of the stiction failed micro-cantilever beams. Using dynamic fracture models in cooperation with the modal analysis, a procedure to predict the onset of de-cohesion of the adhered cantilever beam is established. Specifically, de-cohesion is initiated when the dynamic energy release rate exceeds a critical interface fracture energy, which is known to control adhesion. The competition between stored elastic energy and adhesive forces has naturally led to the application of fracture mechanics models, which introduce a critical interface adhesion energy that must be overcome to initiate debonding [1-4]. This framework is attractive because of both its simplicity and its ability to predict failure using a single parameter characterizing the interface. This is a critical advantage since many systems (and adhesion mechanisms) involve nanoscale forces and displacements that are difficult to measure directly. The principal motivation for the present analysis is to explore the possibility of using probes or electrodynamic forces to induce vibrations that promote the release of adhered structures. It is the goal of this work to identify parameter combinations that lead to *initiation* of stick release. These approaches may have important advantages in scenarios where alternative prevention or repair strategies are ineffective or prohibitively expensive. Electrodynamically induced vibrations generated using the functionality of the chip itself could be combined with laser pulse heating, which uses rapid heating to promote debonding and restore function [5-7].



Reliability, Packaging, Testing, and Characterization of MEMS/MOEMS IV,
edited by Danelle M. Tanner, Rajeshuni Ramesham, Proc. of SPIE Vol. 5716
(SPIE, Bellingham, WA, 2005) · 0277-786X/05/$15 · doi: 10.1117/12.590849

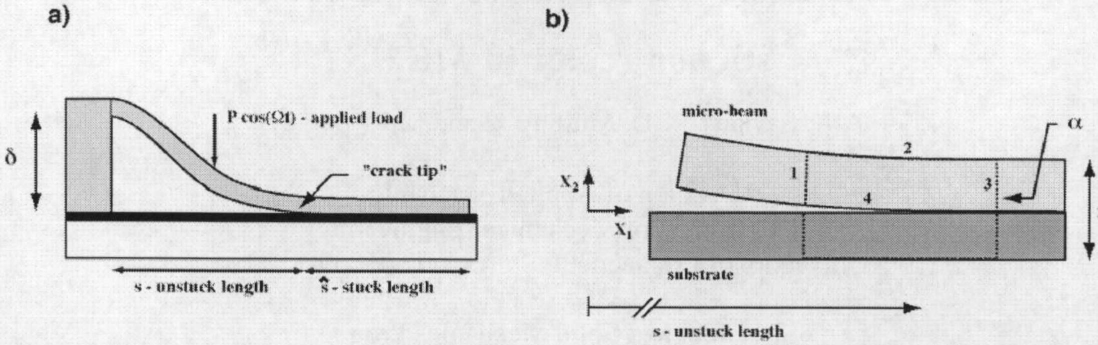


**Figure 1**: **a)** Schematic of stiction failed single cantilever beam adhered to the substrate, shown is acted upon by a dynamic load. **b)** Schematic of a beam adhered to the substrate, treated as a fracture problem, showing crack tip activity

## 2. ANALYTICAL MODELS

Two models are developed to predict the initiation of de-cohesion of adhered cantilevers, which are subjected to harmonic uniform pressures loads. A linear vibration model for the response of the beam (presented first) is used as input to the dynamic fracture model (presented second), which yields the dynamic energy release rate. These models are used together in Section 3 to predict the onset of de-cohesion. Figure 1a shows a cantilevered micro-beam deformed into an s-shape due to adhesion with the substrate. The rectangular beam has length $L$, an unstuck length of $s$, depth $b$, and thickness $h$. The gap between the free standing beam and the substrate is $\delta$. A transverse, harmonic point load (shown) or a harmonic uniform pressure load with frequency $\Omega$ is applied to the beam.

### 2.1. Vibration Model

A stiction failed MEMS cantilever beam as shown in the Figure is subjected to a time varying uniformly distributed pressure load expressed as:

$$P(x,t) = P(x)\cos(\Omega t), \tag{1}$$

where $P(x) = P$. The total deflection is a superposition of the dynamic response and the (static) equilibrium position with zero externally applied load. The static position of the beam, $w_o(x)$, is dictated by elementary beam theory, clamped boundary conditions and the condition that $w_o(s) = \delta$. This renders the following initial deflection (with zero applied load) of the beam

$$w_o = \delta\left(3\left(\frac{x}{s}\right)^2 - 2\left(\frac{x}{s}\right)^3\right). \tag{2}$$

This is used as the reference position for the dynamic analysis, which includes the effect of the externally applied load. Modal analysis is used to obtain a solution to the governing dynamic beam equation, given by:

$$m\ddot{w} + c\dot{w} + EIw^{IV} = P(x)\cos(\Omega t), \tag{3}$$

where $m$ is the mass per unit length, $c$ is the damping constant, $EI$ is the bending rigidity, $w$ is the deflection relative to the static position, and dots and primes refer to derivatives with respect to time and space, respectively. Note that $w$

represents the deflection arising from the applied load, and does not include the initial deflection arising from the gap separation. A separable solution of the following form is sought:

$$w(x,t) = \sum_{i=1}^{\infty} A(t)\Psi_i(x), \tag{4}$$

Where

$$\Psi_i(x) = \frac{1}{2}\left[\lambda_i e^{\beta_i x} + \kappa_i e^{-\beta_i x}\right] - \cos(\beta_i x) + \alpha_i \sin(\beta_i x), \tag{5}$$

is the $i^{th}$ mode shape of a clamped-clamped beam and $\lambda_i$, $\kappa_i$ and $\beta_i$ are tabulated values [8]. Substituting this separable solution in the Equation 3 and invoking orthogonality renders a linear, second order, constant coefficient ordinary differential equation for the $i^{th}$ modal amplitude. The total solution is a superposition of the transient and steady state amplitude and is given by:

$$w(x,t) = \sum_{i=1}^{\infty} \left[A_i^{\,t}(t) + A_i^{\,ss}(t)\right]\Psi_i(x). \tag{6}$$

The constants arising in the transient solution are found by assuming zero deflection and zero velocity with respect to the static deflection, as initial conditions.

### 2.2. Fracture Model

In the fracture mechanics model used to predict the onset of de-cohesion between the beam and the fixed, semi-infinite substrate, the 'crack tip' occurs at the point of separation of the two surfaces, as indicated in Figure 1b In this work, a dynamic form of the energy release rate, $G_d$, which includes inertial effects, is derived from the energy flux integral approach described in detail by Freund [9]. The goal is to determine the instantaneous rate of energy flow through an arbitrary control volume containing the crack tip. The boundary of this volume is denoted as $\alpha$ and is shown in Figure 1b. The energy flux is obtained by taking a dot product between the Newton's second law, $\sigma_{ji},_j - \rho u,_{tt} = 0$, and the velocity field, $\partial u_i / \partial t$, and integrating around the boundary. This leads to a general expression for $F$, the energy flow into $\alpha$ towards the crack tip:

$$F(\alpha) = \int_{\alpha} \left[\sigma_{ij} n_j \frac{\partial u_i}{\partial t} + (U + T)\dot{s} n_j\right] d\alpha\,, \tag{7}$$

where $\sigma_{ij}$ is the stress field, $n_j$ is the outer normal to the boundary $\alpha$, $\dot{s}$ is the velocity of the crack tip, and $d\alpha$ is an element of the boundary. $U$ is the stress work density, given by:

$$U = \int_{-\infty}^{t} \sigma_{ij} \frac{\partial^2 u_i}{\partial t \partial x_j} dt, \tag{8}$$

and $T$ is the kinetic energy density, given by:

$$T = \frac{1}{2}\rho \frac{\partial u_i}{\partial t}\frac{\partial u_i}{\partial t}. \tag{9}$$

The dynamic energy release rate is related to the flux integral, Equation (7), by the relation [9]:

$$G_d = \frac{F(\alpha)}{\dot{s}}. \tag{10}$$

Here, $G_d$ represents the energy release rate arising from the applied dynamic load and is determined from the deflections relative to the static equilibrium position. The contribution arising from the initial static deflection caused by the initial gap separation, $G_s$, is superposed in the final step of the derivation.

For the particular problem of a micro-cantilever stuck to a semi-infinite substrate, $F(\alpha)$ is calculated over the boundary shown in Figure 1b. The energy flux integral is easily evaluated within the framework of 2-D, linear elastic Euler-Bernoulli beam theory, which describes the transverse deflection of the neutral axis (at $x_2 = h/2$ as $u_2 = w(x_1,t)$).

Several observations simplify the evaluation of the integral. First, no energy flows through $\alpha$ from the substrate, since it is static and unstressed. In the beam, there are four areas through which energy might flow, and they are as labeled in Figure 1b. Ahead of the crack tip,(side 3 of $\alpha$) where $x_1 = s^+$, the curvature and velocity are both zero. Thus, there is no contribution to the energy flux from this side. In addition, there is no contribution along sides 2 or 4, since these are traction free surfaces and $n_1 = 0$. This leaves only the flux along side 1, located at $x_1 = s^-$. Using these simplifications, and elementary calculus the individual terms of the Equation (7) are evaluated to obtain the dynamic energy release rate given as [9]:

$$G_d = \frac{F(\alpha)}{\dot{s}} = \frac{6M^2(s^-,t)}{Eh^3}\left(1 - \frac{\dot{s}^2}{c_o{}^2}\right), \tag{11}$$

where $M(s^-,t)$ is the dynamic moment at the crack tip, E is the modulus of elasticity of the beam, h is thickness, $\dot{s}$ is the crack tip velocity and $c_0$ shear speed. Since the objective is to examine the *initiation* of crack propagation, the term $(\dot{s}/c_o)^2$ is zero and maybe omitted from Equation (11). Evaluation of Equation (11) requires an expression for the dynamic moment at the crack tip arising from the periodic applied load, which was developed in Section 2.1 and is given by $M(s^-,t) = EIw''(s^-,t)$.

De-cohesion is initiated when the net energy release rate is equal to the interface toughness, i.e. $G_{total} = \Gamma_i(\dot{s})$. The net energy release rate is given by the superposition of static and dynamic terms:

$$G_{total} = G_s + G_d, \tag{12a}$$

where $G_s$ is the energy release rate arising only from the initial gap separation (i.e. the initial deflection), given by [3-6]:

$$G_s = 18\frac{EI\delta^2}{bs^4}. \tag{12b}$$

Hence, the first term does not include the effect of the externally applied harmonic loading. The second term is calculated using deflections referenced to the initial position.

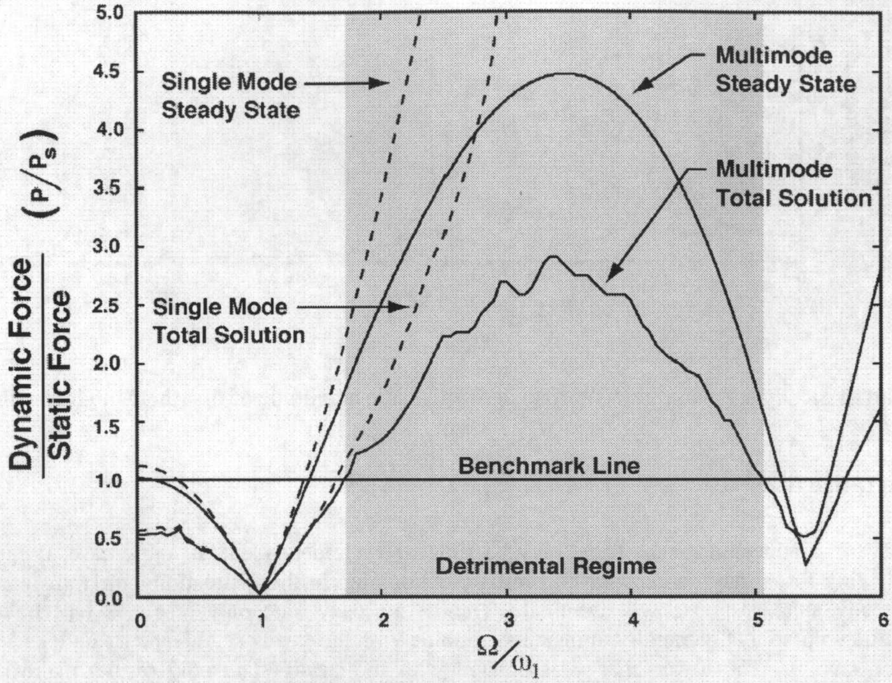


**Figure 2:** Prediction of dynamic force required to initiate de-cohesion of beam from the substrate for a distributed loading condition for single and multimode cases.

## 3. RESULTS

A uniform pressure load, where $P(x) = P$, is considered. This is motivated by the idea that harmonic electrodynamic pressures may be used to excite the beam. Strictly speaking, an electrodynamic pressure generated between the deflected beam and substrate would not be uniform, as it depends on the separation between the cantilever and the substrate. However, uniform pressure loading provides general insight into the distributed load problem. It is also important to note at this point, that the loading scenario chosen for the analysis is completely arbitrary. Various gap dependent loading scenarios may be considered to describe the complexities of the actual actuation force.

### 3.1. Distributed load

Figure 2 shows the $(\Omega, P)$ parameter combinations leading to debond initiation for the uniformly distributed, harmonic excitation. It shows the single and multimode solutions for the steady state only response and total response (steady state + transient). These curves can be split in three distinct zones i.e. first is the zero frequency zone, second is the zone near the resonant frequency and the third zone is between the resonant frequencies.

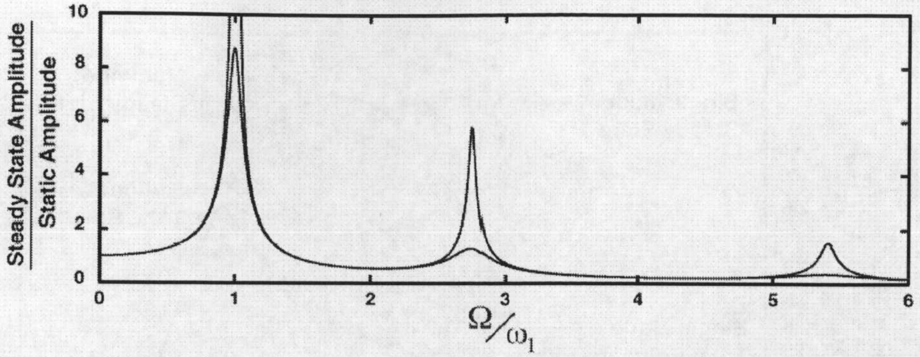


**Figure 3:** Variation of Steady state amplitude normalized with static amplitude of first three modes, with the normalized frequency.

#### 3.1.1. Steady state behavior

It is possible that some adhesion mechanisms may be time or cycle-dependent. In these case, numerous successive cycles of large driving force may be necessary to initiate debonding. In these situations, the transients will have died away and the steady state response will dominate. Hence, a steady-state *only* response will be considered first. However, it should be noted that, generally, transients combine with the steady state response and, as a result the steady state only will be smaller. The lower energy associated with the steady state only results make it a conservative approach.

Two steady state results are shown in Figure 2– one with a single mode retained and second with 3 modes retained. First, consider the single mode steady state solution. At low frequencies, the force required to initiate peeling is approximately half of the required static force to cause peeling, which clearly does not capture the true nature of the structural response. To understand this behavior one needs to look at the multimode response (retaining three modes), which asymptotes to the static value at zero frequency. As the frequency is increased from zero, the single mode curve decreases until $\Omega / \omega_1 = 1$. The reduced force amplitude required for debond initiation near the first natural frequency can be attributed to the structural response of the beam, as shown in Figure 3. This shows the variation of the steady state displacement amplitude of the load point as a function of the normalized frequency. The results in the figure are normalized relative to the static displacement amplitude and the first natural frequency. For illustrative purposes, two different damping cases are shown: $\zeta = 0.01$ and $\zeta = 0.05$. This behavior explains the results shown in Figure 2; as the displacement amplitude increases near resonance $(\omega = \omega_1)$, the energy supplied to the crack tip for debonding increases. Hence, in the single mode model, the forcing amplitude required to initiate debonding decreases as the first resonant frequency is approached. As the frequency is increased beyond $\Omega/\omega_1 = 1$, the required force increases without bound.

Next, consider the multi-mode case retaining 3 modes. As $\Omega/\omega_1 \to 0$, the dynamic force required approaches the static peeling force. If the forcing frequency is increased, the force amplitude drops at the 1st resonant frequency and then rises again. One might expect similar dips at $(\omega = \omega_2)$ and $(\omega = \omega_3)$. Curiously, there is no drop in the multimode solution at the second frequency. For the purely symmetric applied load, the anti-symmetric second mode cannot contribute. As a result, the second mode (or any asymmetric mode, for that matter) cannot be excited by this loading function. Because there is no dip near $(\omega = \omega_2)$, the required load (in this region) exceeds the static peeling force $P_s$, given by the horizontal line at $P/P_s = 1$. This line serves as a benchmark, indicating whether vibrations are an improvement over a simple static peeling load. The range of frequencies for which $P/P_s > 1$ is referred to as a 'detrimental regime' because, in these regimes, vibrations actually are a detriment (relative to the static case) to the stick release process.

### 3.1.2. Transient behavior

Now consider including the transient behavior (see Equation 6) for both the single and multi-mode (total) responses. The single mode total solution shows the same general trends as the steady-state only single mode solution but the force required for debonding is smaller at any excitation frequency. This is because $G_{total}$ exceeds $\Gamma_i$ in the transient regime of the motion. Clearly the steady-state only solution is conservative, as it tends to over-predict the minimum load required for debonding. The multi mode result corresponds to the lowest curve in Figure 2. Again, this curve shows similar trends to the steady-state only curve. Near the resonances, less force is required. However, the total multi-mode result is *much* lower than the steady-state (only) multi-mode result. Both curves experience a drop in the required force as the first resonance is approached. However, there is no drop in the require force at the second resonant frequency – only at the first and third frequencies. The total solution results do not approach the static value at low frequencies, since transients continue to play a significant role. Near the first resonance, the required force drops. Like the steady-state only results, the total solution also does not dip near the second resonant frequency. In fact, the required force is larger than the static force (for frequencies indicated by the gray regions). The reason for this is similar to the discussion made for the steady state behavior which is attribute to the asymmetric loading.

## 4. CONCLUSION

Using this model, critical combinations of the excitation frequency and force level $(\Omega, P)$, which initiate debonding, have been identified. It is clearly demonstrated that when the excitation frequency is near any natural frequencies of the adhered beam, the required force is reduced significantly. This indicates lower power requirements to achieve stiction release near resonant frequencies making it an attractive non-invasive technique for stick repair in MEMS devices.

## REFERENCES:


1. E. E. Jones, M. R. Begley, and K. D. Murphy., "Adhesion of Micro-Cantilevers Subjected to Mechanical Point Loading: Modeling and Experiments" *Journal of Mechanics and Physics of Solids*, **51,** 1601-1622, 2003.
2. E. E. Jones, K. D. Murphy, and M. R. Begley, "Adhesion of Micro-Cantilevers Subjected to Mechanical Point Loading: Modeling and Experiments", *Experimental Mechanics*, to appear, 2003.
3. C. H. Mastrangelo, and C. H. Hsu, "A Simple Experimental Technique for the Measurement of the Work of Adhesion of Microstructures," *IEEE Conference Proceedings*, Hilton Head, 1992.
4. M. P. de Boer, and T. A. Michalske, "Accurate Method for Determining Adhesion of Cantilevers Beams," *Acta Materialia*, **48**, 4531-4541, 2000.
5. N. C. Tien, S. Jeong, L. M. Phinney, K. Fushinobu, J. Bokor, "Surface Adhesion Reduction in Silicon Microstructures Using Femotosecond Laser Pulses", *Applied Physics Letters*, **66**(2), 197-199, 1995.
6. K. Fushinobu, L. M. Phinney, and N. C. Tien, "Ultrashort-Pulse Laser Heating of Silicon to Reduce Microstructure Adhesion", *Internation Journal of Heat and Mass Transfer*, **39**(15), 3181-3186, 1996.
7. L. M. Phinney, J. W. Rogers, "Pulsed Laser Repair of Adhered Surface –Micromachined Polycrystalline Silcon Cantilevers", *Journal of Adhesion Science and Technology*, 17(4), 603-622, 2003.
8. L. B. Freund, *Dynamic Fracture Mechanics*. 1990, Cambridge: Cambridge University Press.
9. C. T. Chang, R. C. Roy Jr., "Normal Modes of Uniform Beams". Journal of Engineering Mechanics Div ASCE, 1027-1031, 1969.